

# Analysis of distortions in the velocity profiles of suspension flows inside a light-scattering medium upon their reconstruction from the optical coherence Doppler tomograph signal

A.V. Bykov, M.Yu. Kirillin, A.V. Priezzhev

**Abstract.** Model signals from one and two plane flows of a particle suspension are obtained for an optical coherence Doppler tomograph (OCDT) by the Monte-Carlo method. The optical properties of particles mimic the properties of non-aggregating erythrocytes. The flows are considered in a stationary scattering medium with optical properties close to those of the skin. It is shown that, as the flow position depth increases, the flow velocity determined from the OCDT signal becomes smaller than the specified velocity and the reconstructed profile extends in the direction of the distant boundary, which is accompanied by the shift of its maximum. In the case of two flows, an increase in the velocity of the near-surface flow leads to the overestimated values of velocity of the reconstructed profile of the second flow. Numerical simulations were performed by using a multiprocessor parallel-architecture computer.

**Keywords:** Monte-Carlo method, light scattering, coherence length, optical coherence Doppler tomography.

## 1. Introduction

Optical coherence Doppler tomography (OCDT) is a modern non-invasive high-resolution optical method, which can find wide applications for visualisation of the internal structure and dynamics of various media and objects [1, 2]. At present this method is more often used in biomedical investigations for the visualisation of the structure of biological tissues and the blood flow dynamics both in physical models and living objects [3, 4]. In particular, optical coherence Doppler tomography is used for clinical diagnostics of pathologic changes in the eye and skin tissues and mucosa developed during various diseases [5]. However, this method is continuously being progressed and, therefore, the study of its potential capabilities is still of current interest. One of the efficient methods of such a

study is the numerical simulation of the signal from an optical coherence Doppler tomograph (OCDT) and the reconstruction from this signal of sought for parameters of an object mimicking the initial system. In particular, the Monte-Carlo method of statistical simulations has received wide applications in such studies [6].

The OCDT is based on a Michelson interferometer. In the reference arm of the interferometer, a scanning mirror is placed, and an object is placed in the object arm. As a broadband light source, a superluminescent diode with the coherence length of the order of ten micrometers is used, as a rule. A high spatial resolution during the longitudinal scan is achieved due to the fact that the reference radiation interferes dynamically only with that fraction of radiation backscattered from the optical inhomogeneities within the object for which the optical path difference of the waves is smaller than the coherence length of the radiation source. Thus, the output signal of the tomograph obtained during one scan over the object depth (the so-called A scan) is a superposition of the sequence of interference patterns with the modulation frequency proportional to the scanning rate of the reference mirror.

The amplitude of each pattern is determined by the relative refractive index, size, and shape of the corresponding inhomogeneity. The waves scattered by moving particles make contributions to the signal with the additional Doppler frequency shift, which linearly depends on the velocity of light-scattering particles. Scanning over the flow depth performed by moving the reference mirror allows one to obtain the spatial distribution (profile) of the velocities of moving particles. However, the OCDT signal can contain contributions not only from single-scattered waves but also from multiple-scattered waves [7]. Because of the randomness of the scattering process, the Doppler frequency shifts of these waves are irregular and, therefore, the reconstructed velocity profile can be distorted compared to the real profile.

The aim of this paper is to elucidate the degree and type of distortions of the flow velocity profile reconstructed from the OCDT signal caused by multiple scattering of light in the medium surrounding the flow and also to study the possibility of reconstruction of the velocity profile of the second, deeper flow.

## 2. Simulated setup and the object under study

The simulated setup is identical to that we described earlier in [7, 8] and is the OCDT system based on a Michelson interferometer with a 822-nm superluminescent diode radiation source with the coherence length  $l_{\text{coh}} = 15 \mu\text{m}$ . The

A.V. Bykov, M.Yu. Kirillin Department of Physics, M.V. Lomonosov Moscow State University, Vorob'evy gory, 119992 Moscow, Russia; e-mail: sasha5000@tut.by, mkirillin@yandex.ru;

A.V. Priezzhev Department of Physics, International Laser Center, M.V. Lomonosov Moscow State University, Vorob'evy gory, 119992 Moscow, Russia; e-mail: avp2@mail.ru

Received 5 July 2005

Kvantovaya Elektronika 35 (11) 1079–1082 (2005)

Translated by M.N. Sapozhnikov

scanning velocity of the mirror in the reference arm of the interferometer is  $V_m = 12 \text{ mm s}^{-1}$ . The angle between the laser beam incident on the object and the flow propagation direction is  $75^\circ$ . We studied one or two flat suspension flows separated by the distance  $D = 100 \text{ }\mu\text{m}$  inside a stationary scattering medium. The moving liquid is simulating a flat blood layer, which is treated as a suspension of non-aggregating erythrocytes with the volume concentration (hematocrit) of 35%. This concentration is close to the physiological concentration of erythrocytes in the human small blood vessels. The parameters of the model of the surrounding medium correspond to the parameters of the 2% intralipid solution. Intralipid is a suspension of lipid particles. The optical properties of the 2% intralipid solution are close to those of the skin [9] and this suspension is often used in experiments to mimic the human skin. The optical parameters of the media (scattering and absorption coefficients  $\mu_s$  and  $\mu_a$ , the anisotropy factor  $g$ , the refractive index  $n$ , and the transport length  $l_{tr} = [\mu_a + \mu_s(1 - g)]^{-1}$  characterising the distance at which a photon ‘forgets’ its initial direction) chosen for blood [10] and intralipid [11, 12] are presented in Table 1.

**Table 1.** Model parameters for blood and intralipid.

Component of the medium	$\mu_s/\text{mm}^{-1}$	$\mu_a/\text{mm}^{-1}$	$g$	$n$	$l_{tr}/\text{mm}$	References
Blood (35%)	57.3	0.82	0.977	1.4	0.47	[10]
Intralipid (2%)	5.4	0.002	0.7	1.36	0.62	[11, 12]

In the model of a medium with one flow (Fig. 1a), the position depth  $L$  of the blood layer in intralipid was varied from 50 to 300  $\mu\text{m}$ , which corresponds to the physiological position depths and blood vessel thicknesses. The velocity profile in the blood flow layer was assumed parabolic with the maximum velocity of  $5 \text{ mm s}^{-1}$ , which is close to its value for the real velocity distribution in a capillary. In the model of a medium with two flows (Fig. 1b), the distance  $D$  between the flows and the position depth  $L$  of the first layer were varied.

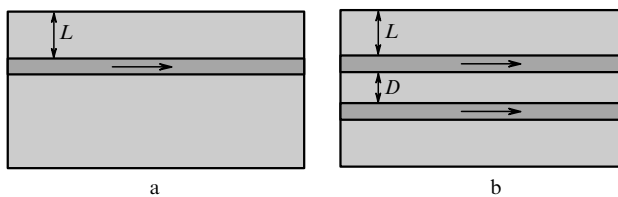


**Figure 1.** Schemes of a simulated object with one (a) and two (b) flows.

It was assumed that the velocity profile in the second flow was parabolic, with the constant maximum velocity  $V_2 = 5 \text{ mm s}^{-1}$ , while the maximum velocity  $V_1$  of the first flow, which also had a parabolic velocity distribution, was varied from 0 to  $10 \text{ mm s}^{-1}$ .

### 3. Algorithm for signal simulation

We modified the algorithm for simulating the OCDT signal [7] for calculations using multiprocessor computers with parallel architecture. This algorithm consists of two stages. First, the trajectories of single photons and their Doppler

frequency shifts are calculated by using the standard Monte-Carlo algorithm with the phase Henyey–Greenstein phase function [13]. Then, the optical mixing of photons incident on a photodetector from the reference and object arms is simulated in each time interval of the scan with the help of the interference formula

$$I = (N_r N_s)^{1/2} \cos \left[ \left( \frac{2\pi}{\lambda} + \frac{2\pi \Delta f}{V_m} \right) \Delta l \right] \exp \left[ - \left( \frac{\Delta l}{l_{\text{coh}}} \right)^2 \right]. \quad (1)$$

Here,  $N_r$  and  $N_s$  are the numbers of photons incident on a photodetector from the reference and object arms, respectively, at the given time interval with the given path difference;  $\Delta f$  is the average Doppler frequency shift for photons coming from the object arm for the same time interval; and  $\Delta l$  is the optical path difference for interfering waves.

Photons scattered within the angular aperture of  $6^\circ$  with respect to the strictly backward direction are assumed detected. The angle between this direction and the normal to the surface of the medium under study is  $15^\circ$ . The velocity in each scan interval was determined from the calculated Doppler shifts by the expression

$$V = \frac{\Delta f \lambda}{2n \cos \theta}, \quad (2)$$

where  $n$  is the refractive index of the medium and  $\theta$  is the angle between the incident laser beam and the flow velocity vector.

### 4. Results of simulation and discussion

Monte-Carlo simulation of the light propagation in a strongly scattering medium requires a long time. Thus, the simulation of only one OCDT signal by using a conventional PC, when the parameters of a medium correspond to real biological systems, can be quite long since the OCDT is highly selective to backscattered photons [6]. To substantiate the use of multiprocessor computers with parallel architecture for calculating the OCDT signals, we compare several signals from a medium with two flows, calculated for the following parameters of the medium:  $L = 50 \text{ }\mu\text{m}$ ,  $D = 100 \text{ }\mu\text{m}$ , and  $V_1 = 10 \text{ mm s}^{-1}$ .

To obtain the result presented in Fig. 2, 500 million photons were used. The calculation time by using an AMD Athlon 2 GHz PC was approximately eight hours. Figure 2b presents the result of calculations for 10 billion photons. This result was obtained with the help of a 10-processor ILC MSU computer (IBM cluster, 2x-Xenon 2600) during the same time. In Fig. 2b, unlike Fig. 2a, the velocity distribution in the second, deeper flow is distinctly observed. Also, one can see that the parasitic signal, which we call the ‘Doppler noise’ (see below), as if corresponding to nonzero velocities, which supposedly exist outside flows, is characterised by certain values. These values cannot be found from the data presented in Fig. 2a. All the results presented below were obtained with the multiprocessor computer by using 10 billion photons.

Consider the above-described system with one flow at different flow position depths. The results of simulations of this system are presented in Fig. 3. One can see that, as the position depth of the layer under study increases, the maximum of the reconstructed velocity profile shifts to

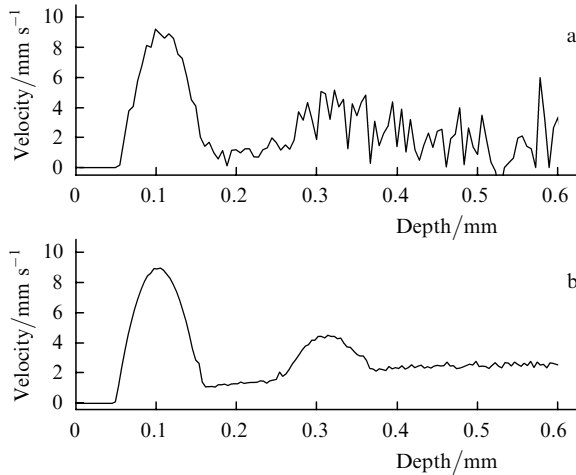


**Figure 2.** Comparison of velocity distributions in a scattering medium with two immersed flows reconstructed by the OCDT signal and calculated by using a PC (a) and a multiprocessor computer (b).

the region of larger depths and its intensity decreases. This is explained by the fact that the number of photons carrying reliable information on the flow decreases with increasing the position depth. Photons coming from a larger depth have more complicated and long trajectories, thereby affecting destructively the profile reconstruction.

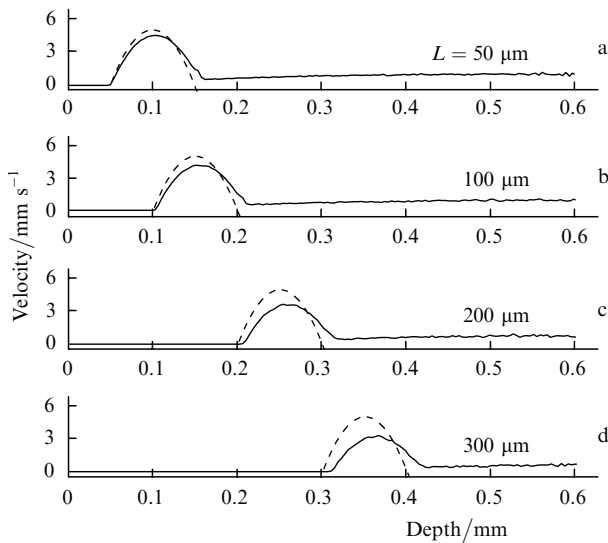


**Figure 3.** Comparison of Poiseuille's (real) profile (dashed curves) and the flow velocity profiles simulated by the Monte-Carlo method (solid curves) in a blood layer in a scattering medium at different flow position depths.

Figure 4 presents the dependences of the maximum velocity of the reconstructed flow and the position of the maximum of the velocity profile on the flow position depth. One can see that in the region behind the flow, the nonzero (parasitic) velocities (Doppler noise) are observed, which appear because photons coming from this region at least twice have crossed the flow and have acquired additional Doppler shifts. Obviously, this noise will be manifested upon the detection and reconstruction of the velocity profiles of the flows positioned deeper. The presence of the Doppler noise in the study of flows immersed into a

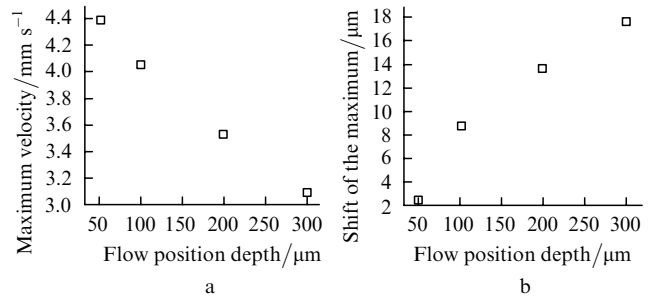


**Figure 4.** Dependences of the maximum flow velocity (a) and the shift of the maximum (b) of the reconstructed velocity profile on the flow position depth.

strongly scattering medium was experimentally demonstrated for model skin phantoms [14]. The results presented in [14] are in qualitative agreement with our results presented in Fig. 3.

Then, we studied the effect of the Doppler noise on the accuracy of determining the flow velocity profile in a system of two parallel unidirectional flows. The results of simulations for this system for the depth of the first flow  $L = 50 \mu\text{m}$  and the separation between the flows  $D = 100 \mu\text{m}$  are shown in Fig. 5. One can see that, as  $V_1$  increases, the velocity of the second reconstructed flow also increases. This occurs because the real velocity of this flow is overlapped by the Doppler noise from the first flow, which directly depends on the first-flow velocity. Simultaneously with the increase in the reconstructed velocity, the boundaries of the second flow are blurred. For a different separation between the flows ( $D = 60 \mu\text{m}$ ) and the invariable position of the first flow ( $L = 50 \mu\text{m}$ ), the reconstructed maximum velocity of the second flow proved to be greater than for  $D = 100 \mu\text{m}$ . This is explained by the effect described above (the maximum velocity of the reconstructed profile decreases with

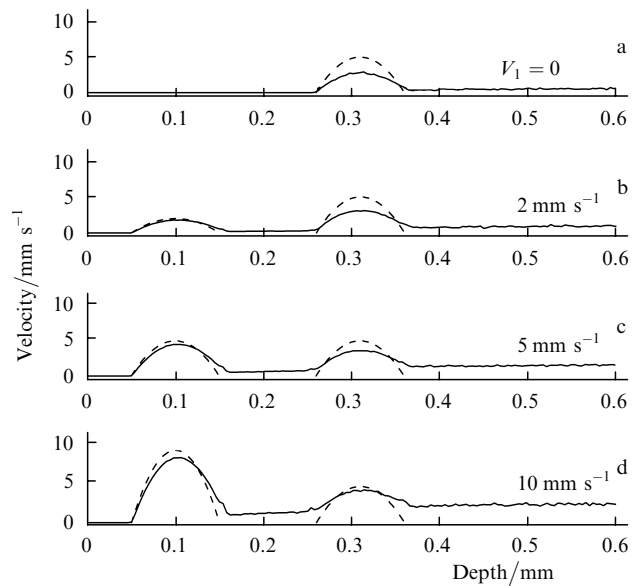


**Figure 5.** Comparison of Poiseuille's (real) profile (dashed curves) and the flow velocity profiles simulated by the Monte-Carlo method (solid curves) for two unidirectional blood flows in a scattering medium separated by the distance  $D = 100 \mu\text{m}$  for different maximum velocities  $V_1$  of the first flow.

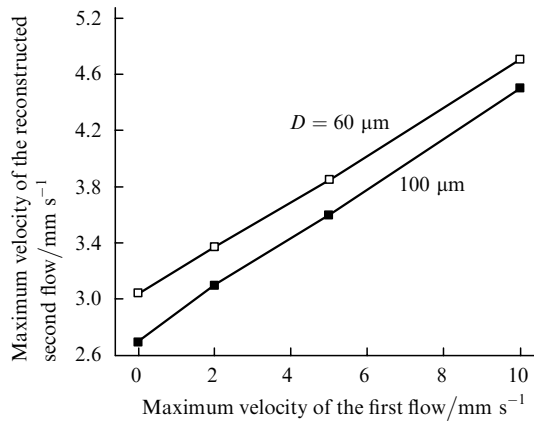


**Figure 6.** Dependences of the maximum velocity of the reconstructed profile of the second flow on the maximum velocity of the first flow for the flow separation  $D = 60$  and  $100 \mu\text{m}$ .

increasing the flow position depth). The obtained results are compared in Fig. 6.

## 5. Conclusions

We have analysed the effect of the position depth of a particle suspension flow in a light-scattering medium on the velocity profile reconstructed from a signal of the optical coherence tomograph. The optical properties of the moving suspension mimicked the properties of blood considered as a suspension of noninteracting optically soft particles. It was assumed that the real flow profile corresponded to the Poiseuille's flow. The optical properties of the medium surrounding the flow simulated the averaged properties of the human skin. Thus, the physical model used in the paper simulated as a whole the blood flow in a skin layer. Our analysis has shown the following. As the position depth of the bloodstream increases, the velocity profile reconstructed by the OCDT signal is distorted in such a way that (i) the reconstructed velocities prove to be lower than those specified in the model (the maximum velocity at the depth  $300 \mu\text{m}$  is one and a half times lower than the real velocity specified in the model) and (ii) the reconstructed profile extends in the direction of the distant boundary and its maximum shifts. This shift is caused by multiple scattering in a stationary medium and achieves the value of  $18 \mu\text{m}$  at the flow position depth equal to  $300 \mu\text{m}$ .

Analysis of the influence of the velocity of the near-surface flow on the accuracy of measuring the velocity of deeper flows showed that, as the velocity of the near-surface flow increased, the velocity of the reconstructed profile of the second flow also increased. This occurs due to the presence of the Doppler noise from the first flow. As the position depth of the second flow increases, the reconstructed value of its velocity also increases with increasing the first-flow velocity. However, because of a decrease in the reconstructed velocity with increasing the flow position depth, the reconstructed velocity of the second flow will be lower than in the case when the second flow is located closer to the surface.

**Acknowledgements.** This work was supported by the Program 'Leading Scientific Schools of Russia' (Grant No. 2071.2003.4).

## References

1. Milner T.E. et al., in *Handbook of Optical Coherence Tomography*. Ed. by B.E. Bouma, G.J. Tearney (New York: Marcel Dekker, 2002) p. 203.
2. Chen Z., Zhao Y., Srinivas S.M., Nelson J.S., Prakash N., Frostig R.D. *IEEE J. Sel. Top. Quantum Electron.*, **5** (4), 1134 (1999).
3. Chen Z., in *Handbook of Coherent Domain Optical Methods*. Ed. by V.V. Tuchin (Kluwer: Kluwer Academic Publ., 2004) Vol. 2, p. 315.
4. Proskurin S.G., Yonghong He, Wang R.K. *Physics in Medicine and Biology*, **49**, 1265 (2004).
5. Leitgeb R.A., Schmetterer L., Drexler W., Fercher A.F., Zawadzki R.J., Bajraszewski T. *Opt. Express*, **11** (23), 3116 (2003).
6. Lindmo T., Smithies D.J., Chen Z., Nelson J.S., Milner T.E. *Physics in Medicine and Biology*, **43**, 3045 (1998).
7. Bykov A.V., Kirillin M.Yu., Priezzhev A.V. *Kvantovaya Elektron.*, **35**, 135 (2005) [*Quantum Electron.*, **35**, 135 (2005)].
8. Hast J., Prykari T., Alarousu E., Myllyla R., Priezzhev A.V. *Proc. SPIE Int. Soc. Opt. Eng.*, **4965**, 66 (2003).
9. Troy T.L., Thenmadil S.N. *J. Biomedical Opt.*, **6** (2), 167 (2001).
10. Roggan A., Friebel M., Dorschel K., Hahn A., Müller G. *J. Biomedical Opt.*, **4** (1), 36 (1999).
11. Flock S.T., Jacques S.L., Wilson B.C., Star W.M., van Gemert M.J.C. *Lasers in Surgery and Medicine*, **12**, 510 (1992).
12. Van Staveren H.G., Moes C.J.M., van Marle J., Prahl S.A., van Gemert M.J.C. *Appl. Opt.*, **30**, 4507 (1991).
13. Yaroslavsky A.N., Yaroslavsky I.V., Goldbach T., Schwarzmaier H.-J. *J. Biomedical Opt.*, **4** (1), 47 (1999).
14. Moger J., Maicher S.J., Winlove C.P., Shore A. *J. Phys. D: Appl. Phys.*, **38**, 2397 (2005).